Wavelet analysis of shearless turbulent mixing layer

Cite as: Phys. Fluids **33**, 025109 (2021); https://doi.org/10.1063/5.0038132
Submitted: 19 November 2020 • Accepted: 04 January 2021 • Published Online: 18 February 2021

T. Matsushima (松島哲也), K. Nagata (長田孝二) and T. Watanabe (渡邉智昭)

Physics of Fluids ARTICLE scitation.org/journal/phf

Wavelet analysis of shearless turbulent mixing layer

Cite as: Phys. Fluids 33, 025109 (2021); doi: 10.1063/5.0038132
Submitted: 19 November 2020 · Accepted: 4 January 2021 ·
Published Online: 18 February 2021

T. Matsushima (松島哲也), K. Nagata (長田孝二),[a] and T. Watanabe (渡邉智昭)

AFFILIATIONS

Department of Aerospace Engineering, Nagoya University, Nagoya, Japan

[a]Author to whom correspondence should be addressed: nagata@nagoya-u.jp

ABSTRACT

The intermittency and scaling exponents of structure functions are experimentally studied in a shearless turbulent mixing layer. Motivated by previous studies on the anomalous scaling in homogeneous/inhomogeneous turbulent flows, this study aims to investigate the effect of strong intermittency caused by turbulent kinetic energy diffusion without energy production by mean shear. We applied an orthonormal wavelet transformation to time series data of streamwise velocity fluctuations measured by hot-wire anemometry. Intermittent fluctuations are extracted by a conditional method with the local intermittency measure, and the scaling exponents of strong and weak intermittent fluctuations are calculated based on the extended self-similarity. The results show that the intermittency is stronger in the mixing layer region than in the quasi-homogeneous isotropic turbulent regions, especially at small scales. The deviation of higher-order scaling exponents from Kolmogorov's self-similarity hypothesis is significant in the mixing layer region, and the large deviation is caused by strong, intermittent fluctuations even without mean shear. The total intermittent energy ratio is also different in the mixing layer region, suggesting that the total intermittent energy ratio is not universal but depends on turbulent flows. The scaling exponents of weak fluctuations with a wavelet coefficient flatness corresponding to the Gaussian distribution value of 3 follow the Kolmogorov theory up to fifth order. However, the sixth order scaling exponent is still affected by these weak fluctuations.

I. INTRODUCTION

Turbulence is a widely observed phenomenon in industry and environment, and many studies on turbulent structure and statistics have been conducted. According to turbulence classical phenomenology, i.e., Kolmogorov's self-similarity hypothesis (hereafter denoted as K41),[1] the following scaling law of the p-order longitudinal velocity structure function holds in the range where statistical properties of turbulence depend only on the mean energy dissipation rate of turbulent kinetic energy (TKE) ε and are not affected by viscosity (i.e., in the inertial range),

$$\left\langle (\delta u(r))^p \right\rangle \propto (\varepsilon r)^{\frac{p}{3}}. \tag{1}$$

Here, δu is the velocity increment $u(x+r) - u(x)$ at two points separated by r in the x direction, and $\langle * \rangle$ denotes an ensemble average of $*$. In the case of $p = 2$, Kolmogorov's −5/3 power law in wavenumber space is well known,

$$E = c_K \varepsilon^{\frac{2}{3}} k^{-\frac{5}{3}}. \tag{2}$$

Here, E is the energy spectrum, c_K is Kolmogorov's constant, and k is the wavenumber. Kolmogorov's −5/3 power law has been verified by experiments of various turbulent flows such as grid-generated turbulence,[2] and values close to the scaling predicted by K41 theory have been obtained.[3] On the other hand, it has been reported since the work of Batchelor and Townsend[4] that the mean energy dissipation rate is not homogeneously distributed but intermittent in scale space. The intermittent nature of turbulence is widely observed in various turbulent flows such as homogeneous isotropic turbulence,[5,6] homogeneous shear flows,[7,8] channel flows,[9,10] a backstep flow,[11] and quantum turbulence.[12] Due to the intermittent nature of the energy dissipation rate and related coherent structure of vortices, scaling exponents of higher-order structure functions deviate from the K41 theory values,[13] which is known as the anomalous scaling. Therefore, it is very important to investigate the intermittent nature of turbulence and incorporate it into the turbulent model and theory. Starting from the refinement theory of K41 by Kolmogorov in 1962,[14] various modified theories that consider the intermittent nature of the energy dissipation rate and the multifractal nature of turbulence have been proposed,[15,16] and for some of them, values close to the scaling obtained by experiments and numerical simulations have been predicted.[17] However, there is still no universal turbulence theory that accurately predicts the scaling for various turbulent flows under various conditions.

From a viewpoint of turbulence modeling, incorporating the results of experiments or direct numerical simulation (DNS) into the model may lead to improvement of the accuracy of the prediction. Since homogeneous isotropic turbulence and homogeneous shear turbulence have a simple condition and free boundary, they have the advantage for easily performing experiments and numerical simulations. Some flow fields observed in industry and environment are, however, often spatially non-uniform. In such an inhomogeneous turbulent flow, multiple scales of vortex could develop, which are transported in space and interact with each other. Thus, it is important to verify the validity of the model for such inhomogeneous turbulent flows. For instance, inhomogeneous turbulence often has small-scale anisotropy,[18] which is not in accordance with Kolmogorov's local isotropic assumption, and large-scale intermittency. The latter feature is characterized by a deviation of probability distribution of large-scale quantity such as velocity fluctuation from a quasi-Gaussian distribution at large fluctuations. The large-scale intermittency also affects the intermittency of energy dissipation and scaling law in inhomogeneous turbulence.[19]

The anomalous scaling has been studied in homogeneous/inhomogeneous shear flows such as a channel flow,[9] a turbulent mixing layer,[20] and a uniform shear flow,[7] as well as grid turbulence,[21–24] where the flow is close to homogeneous and isotropic. In shear flows, there is a shear production of turbulence, and both turbulent production and diffusion may cause intermittency. This study aims to investigate the effect of strong intermittency caused by turbulent kinetic energy diffusion without energy production by mean shear. In order to split the effect of turbulent production and diffusion and to highlight only the effect of turbulent diffusion of vortices in an inhomogeneous flow on anomalous scaling, we use a shearless turbulent mixing layer[18,25–32] in this study. The production of TKE due to mean shear is negligible in a shearless turbulent mixing layer developed by the interaction of two quasi-homogeneous isotropic turbulent regions with different TKEs.[26] The development of TKE depends mainly on the diffusion of TKE. In the mixing layer region, the flatness of turbulent velocity, which is a large-scale statistical property, becomes larger than the Gaussian distribution value of 3.[26] This large-scale intermittency is caused by a penetration of vortices from large to small TKE regions, and there may exist intermittent, large-scale vortex structures in the mixing layer region. Coherent structures in turbulence are associated with a non-Gaussian statistical distribution that induces a deviation from the scaling law predicted by K41. In fact, in homogeneous isotropic turbulence, an intermittent energy dissipation rate and a non-Gaussian statistical behavior have been observed, and they have been studied in connection with coherent structures such as vortex tubes at small scales.[33] To the best of our knowledge, the anomalous scaling has not been investigated in a shearless turbulent mixing layer, and we investigate how strong intermittency caused by a penetration of vortices from a large TKE side affects the anomalous scaling without effects of mean shear.

To this end, we applied an orthonormal wavelet transformation to time series data obtained by hot-wire anemometry in a shearless turbulent mixing layer because it would be difficult to obtain local intermittent information of turbulence with other methods such as Fourier transformation, which converts time signals into frequency information and average local turbulence characteristics into a frequency space using the trigonometric function corresponding to each frequency. Unlike Fourier transformation, wavelet transformation can decompose turbulent signals into coefficients localized in time and frequency (space and scale when Taylor's hypothesis is used) at the same time because wavelets are composed of bases that have both time and frequency information.[34] Wavelets are considered to be a powerful tool for analyzing the multi-scale nature of turbulence and extracting coherent structures contained at a specific space and scale because of their space–scale localization[34] and have been utilized in many studies on turbulence.[23,24,35–41] We use a discrete wavelet transformation to investigate the statistical properties for each scale of the shearless turbulent mixing layer and extract the intermittent fluctuations by a conditional method.[23,24,40] The discrete wavelet transformation consists of orthonormal wavelet bases that can decompose original signals into non-redundant wavelet coefficients.[34,42,43] Since each coefficient represents the information of a turbulent signal at a specific space and scale, we may quantitatively evaluate the intermittency at each scale by the discrete wavelet transformation. The conditional method using the intermittency indicator quantified by the discrete wavelet transformation enables us to split a part that changes statistical properties by strong intermittency from a part that may have universal properties independent of the flow field and Reynolds number.

This paper is organized as follows: In Sec. II A, we briefly describe the grid for generating a shearless turbulent mixing layer and the wind tunnel. In Secs. II B and II C, the discrete wavelet transformation and the extended self-similarity (ESS)[44] are briefly described. In Sec. III, the statistical properties of the shearless turbulent mixing layer are explained, focusing mainly on the wavelet scaling properties. Finally, Sec. IV summarizes conclusions.

II. EXPERIMENT AND DATA ANALYSIS

A. Wind tunnel and grid

The experiment is carried out in an open wind tunnel in Nagoya University. The outline of the wind tunnel with a measurement system is shown in Fig. 1. The wind tunnel has a $0.6 \times 0.6\,\mathrm{m}^2$ cross section, and the length of the measurement section in the streamwise direction is 12 m. The test section has a grid installation part. The contraction part has a ratio of 9:1. The origin of the coordinate system is set at the top of the span-center of the grid. The main flow direction is the x axis, the vertical downward direction is the y axis, and the spanwise direction is the z axis. The maximum wind speed achievable with the wind tunnel is about 30 m/s. The maximum background turbulence intensity in the vicinity of the measured cross section is about 0.81% for a wind speed of 16 m/s at the center of the wind tunnel.

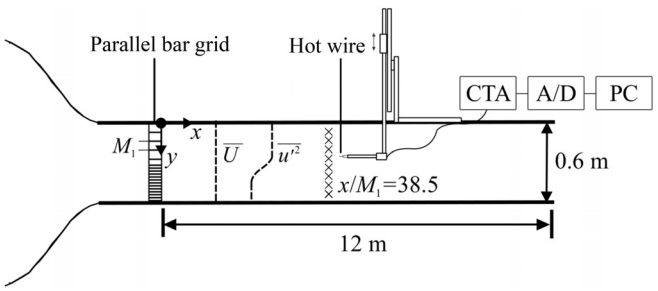

FIG. 1. Schematic of the wind tunnel, flow field, and measurement system.

A hot-wire anemometer (Dantec Dynamics, 90N10 Streamline) with an I-type probe (Dantec Dynamics, 55P11) is used to measure the instantaneous streamwise velocity. The I-type probe is used because of the smaller spatial resolution and lower intrusion than an X-type, following previous studies.[23,24,40] The hot wire consists of a fine tungsten wire with a diameter of 5 μm and a length of 1.25 mm so that the aspect ratio is 250. The overheat ratio is set to 0.8. A standard pitot tube is used to calibrate the hot-wire probe in the test section. The signals are amplified by a signal conditioner installed in the hot-wire anemometer before being sent to the A/D converter (National Instruments, NI-9215). The sampling frequency is f_s = 20 kHz. The number of samples is set to 524 288 at each measurement point and 8 388 608 at some measurement point for wavelet analysis. The sampling number of 524 288 is enough to obtain reliable time-averaged statistics, while more samples are necessary to obtain converged data of the higher-order scaling exponent of the wavelets.

Figure 2 shows the schematic of the grid used for producing the shearless turbulent mixing layer. A parallel bar grid is used to generate two regions of quasi-homogeneous isotropic turbulence with different TKEs following Veeravalli and Warhaft.[26] Table I summarizes the parameters of the grid. The turbulence intensity can be varied by adjusting the mesh width of the grid (i.e., distance between the bars). The mesh widths of the upper and lower grids are M_1 = 31 mm and M_2 = 8.8 mm, respectively. The grid consists of arrays of two stainless steel rods with a square cross section with side lengths of 10 mm and 3 mm. When the mesh width is larger than 10% of the width of the wind tunnel, the development of grid turbulence is affected by the walls of the wind tunnel and reduces the uniformity of the mean flow velocity.[45] In this experiment, this ratio is 5.2% and 1.5% in the upper and lower regions, respectively. Another important design parameter for the grid is the solidity, which is the ratio of the closed area to the total area of the grid and is related to the energy loss due to drag. In order to obtain a uniform mean flow, the solidity must be nearly the same in the two regions. When the solidity exceeds 0.45, jet flows are generated from the grid, and the uniformity of the mean flow is lost.[46] In this study, the solidity is 0.33 for both sides of the grid. The grid width was adjusted by trial and error in order to improve the homogeneity of the mean flow. Consequently, impermeable sponges with a thickness of 0.1 mm are attached to the larger bars. In addition, in order to make the local solidity near the center of the grid closer to other regions, an impermeable sponge with a thickness of 1.8 mm is attached on the lower side of the 10 mm grid in the bottom row. Multiple experiments were performed to determine the solidity and the grid geometry in order to achieve the best homogeneity of the mean flow. Note that in the previous experiment on the shearless turbulent mixing layer by Veeravalli and Warhaft[26] using a similar bar grid, the overall change of the mean streamwise velocity in the vertical direction was ~6% at x/M_1 = 20.6 and the maximum shear rate was ~ 7/s. Therefore, we aimed to achieve uniformity of the mean flow comparable to or higher than theirs by our grid. Finally, as shown in Sec. III A, these values at x/M_1 = 38.5 in this study are less than 1.3% and 6.7/s, respectively.

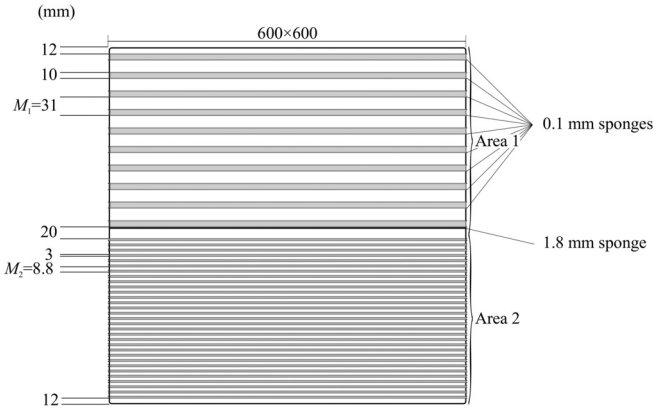

FIG. 2. Schematic of the grid.

TABLE I. Parameters of the grid.

Area	1	2
TKE	Large	Small
Mesh width M_1, M_2 (mm)	31	8.8
Sponge thickness (mm)	0.1	1–4
Bar width w (mm)	10	3
Solidity σ	0.33	0.33
Number of bars	10	31
Geometric center y_{center} (mm)	311	
Center sponge thickness (mm)	1.8	

Flow velocity measurement is performed at x/M_1 = 38.5, where a typical turbulent mixing layer is developed as shown later in Sec. III A. An electric actuator (SUS, XA-50-L) was used for positioning the probe. The positioning accuracy is ±0.02 mm. Table II shows the flow characteristics at different heights (y = 115 mm and 475 mm) at x/M_1 = 38.5. Here, u' is the instantaneous streamwise velocity fluctuation, $\overline{*}$ denotes a time average value of $*$, $u_{rms} = \{\overline{u'^2}\}^{1/2}$ is the streamwise rms velocity, $\lambda = u_{\rm rms}/\{\overline{(\partial u'/\partial x)^2}\}^{1/2}$ is the Taylor microscale, and ν is the kinematic viscosity. Taylor's hypothesis was used to convert spatial to time derivatives with a mean velocity $\overline{U}$.

B. Wavelet analysis

Fourier transformation is a non-local transformation and may hide the information of intermittent turbulence signals. On the other hand, the wavelet transformation can extract the time and frequency

TABLE II. Flow characteristics in the large TKE region (y = 115 mm) and the small TKE region (y = 475 mm) at x/M_1 = 38.5.

y position (mm)	115	475
Mean velocity $\overline{U}$ (m/s)	11.9	11.9
Intensity of streamwise velocity fluctuations $\overline{u'^2}$ (m^2/s^2)	0.42	0.097
Turbulent Reynolds number $Re_\lambda = u_{rms}\lambda/\nu$	165	65
Taylor microscale λ (m)	3.77×10^{-3}	3.57×10^{-3}
Kolmogorov scale η (m)	2.94×10^{-4}	4.43×10^{-4}

information of signals at the same time; therefore, it is possible to investigate the local properties of turbulent signals that depend on the frequency and time or position.[34,47] Here, we briefly describe the discrete wavelet transformation.[34,42,43]

The discrete wavelet transformation, also called a wavelet coefficient, $T_{m,n}$ of signal $x(t)$ is calculated from the inner product of $x(t)$ and the wavelet function $\psi_{m,n}(t)$,

$$T_{m,n} = \int_{-\infty}^{\infty} x(t)\psi_{m,n}(t)dt. \tag{3}$$

The wavelet function $\psi_{m,n}(t)$ is calculated from a mother wavelet $\psi(t)$ by using the parameter m that represents the expansion and contraction of the scale and the parameter n that represents the translation on the time axis. In the discrete wavelet transformation based on 2, the scale m is $m < M$ when the number of samples is $N = 2^M$. Then, information on a discrete scale for every double is obtained,

$$\psi_{m,n}(t) = 2^{-\frac{m}{2}}\psi(2^{-m}t - n). \tag{4}$$

The integral of square of the absolute value of the wavelet must be finite,

$$\int_{-\infty}^{\infty} |\psi(t)|^2 dt < \infty. \tag{5}$$

Also, the Fourier transformation of the wavelet $\hat{\psi}(f)$ must satisfy the following admissible condition:

$$\int_0^{\infty} \frac{|\hat{\psi}(f)|^2}{f} df < \infty. \tag{6}$$

Furthermore, in the non-redundant orthonormal wavelet transformation, the wavelet function is constructed so as to form an orthonormal basis. In this study, the signal is transformed using Haar wavelet,[48] which is an orthonormal wavelet function and has a very good resolution in physical space,

$$\psi(t) = \begin{cases} 1 & \left(0 < t \le \frac{1}{2}\right), \\ -1 & \left(\frac{1}{2} \le t < 1\right), \\ 0 & (\text{otherwise}). \end{cases} \tag{7}$$

We have confirmed that there was little difference in the results regardless of the choice of orthonormal wavelets.

For detecting the intermittency of turbulence, the local intermittency measure (LIM) $I_{m,n}$,

$$I_{m,n} = \frac{T_{m,n}^2}{\overline{T_{m,n}^2}}, \tag{8}$$

has been proposed, which is a ratio of the local energy of the wavelet coefficient at a certain scale m at a certain time to the time-averaged wavelet coefficient.[34] The flatness $F(T_m)$ of the wavelet coefficient at each scale expressed by

$$F(T_m) = \frac{\overline{T_{m,n}^4}}{\overline{T_{m,n}^2}^2} \tag{9}$$

is a quantity that statistically indicates the degree of intermittency at each scale. As a method for extracting large fluctuations, we used the LIM with a threshold s.[23,24,35] The choice of s is arbitrary, and we use a method proposed by Onorato *et al.*[40] to systematically extract intermittent signals. At a certain scale m, s is determined so that the flatness of the wavelet coefficient for fluctuations with the LIM smaller than s is 3, i.e., $\overline{T_{m,n_s}^4}/\overline{T_{m,n_s}^2}^2 = 3$, where n_s represents the time when $I_{m,n} \le s$. Then, the signals with $I_{m,n}$ larger than s are considered to be intermittent fluctuations. Statistics conditioned on $I_{m,n}$ are separately calculated for intermittent fluctuations with $I_{m,n} > s$ and weakly intermittent fluctuations $I_{m,n} < s$. Since the flatness of the wavelet coefficient with fluctuations smaller than s is 3 the probability distribution of the velocity fluctuation is expected to be close to that of homogeneous isotropic turbulence. Note, however, that a flatness factor of 3 does not always mean its probability density function (PDF) is strictly Gaussian.[40] Conditional statistics are obtained from the wavelet coefficients extracted in this way.

The Haar wavelet coefficient is known to be related to the velocity increment,[35,49,50]

$$\overline{|\delta u(r)|} \sim 2^{-\frac{m}{2}}\overline{|T_{m,n}|}. \tag{10}$$

Therefore, the wavelet coefficient can be used to infer the Kolmogorov scaling exponent $\zeta(p)$ in the inertial region[35,36] by the following relation:

$$2^{-\frac{pm}{2}}\overline{|T_{m,n}|^p} \sim r^{\zeta(p)}. \tag{11}$$

C. Extended self-similarity

In this study, we focus on the scaling exponent of the structure function in order to investigate the effect of signals with strong intermittency in the mixing layer region. Here, the extended self-similarity (ESS) proposed by Benzi *et al.*[44] is used to calculate $\zeta(p)$. For flows with a low turbulent Reynolds number, it is difficult to determine the scaling exponent because the inertial range is limited. Benzi *et al.*[44] calculated $\zeta(p)$ by using the q-order structure function of the absolute value of the velocity increment $\overline{|\delta u(r)|^q}$. It is known from the Navier–Stokes equations that the scaling exponent is theoretically 1 for the third order structure function for locally homogeneous isotropic turbulence with a sufficiently large Re_λ. Thus, from the ESS,

$$\overline{|\delta u(r)|^p} \propto \overline{|\delta u(r)|^3}^{\zeta(p)}. \tag{12}$$

By means of ESS, even in the case of grid turbulence with $Re_\lambda = 10$, the scaling law is found in a longer range than that in the case of ordinary structure functions.[22,23] Since the wavelet coefficient is related to the velocity difference, application of ESS to the wavelet coefficient yields the scaling exponent given by

$$2^{-\frac{pm}{2}}\overline{|T_{m,n}|^p} \sim \left(2^{-\frac{3m}{2}}\overline{|T_{m,n}|^3}\right)^{\zeta(p)}. \tag{13}$$

Note that this relationship is an approximation that holds for the Haar wavelet. We could determine the scaling exponents sufficiently up to the sixth order. It should be noted that we also used coiflet 6, which is a quasi-symmetrical and compactly supported orthonormal wavelet, and both its scaling function and wavelet function have vanishing

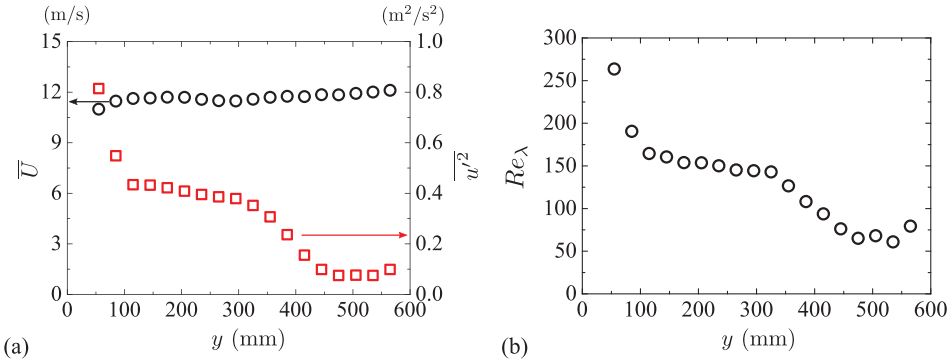

FIG. 3. Vertical distribution of (a) mean velocity (black open circle) and intensity of streamwise velocity fluctuations (red open square) and (b) turbulent Reynolds number.

moments[42,43] as a wavelet function, and confirmed that the main results are not changed.

III. RESULTS AND DISCUSSION

A. Mean and fluctuating field

The vertical (y) distribution of the mean velocity $\overline{U}$ and the intensity of streamwise velocity fluctuations $\overline{u'^2}$ at $x/M_1 = 38.5$ is shown in Fig. 3(a). Except for near the wall at the top and bottom of the wind tunnel (i.e., at $y < 100$ mm and 540 mm $< y$), where the boundary layers develop, the mean velocity is uniform. The mean velocity difference is less than 1.3%, and the maximum shear rate is 6.7/s. These values are comparable or smaller than those in the previous experiment on the shearless turbulent mixing layer,[26] and shear production of turbulence in the present flow is confirmed to be negligible. The vertical distribution of $\overline{u'^2}$, together with Re_λ shown in Fig. 3(b), shows that the typical mixing layer region develops between the large and small TKE regions due to the interaction of quasi-homogeneous isotropic turbulence. Note that Veeravalli and Warhaft[26] have shown that normalized turbulent intensities in the shearless turbulent mixing layer do not vary significantly in the range $33.65 \leq x/M_1 \leq 49.5$ for a similar grid geometry ($M_1 = 31.5$ mm and $M_2 = 9.5$ mm) even at lower Reynolds number than in the present study. Thus, it is expected that the present shearless turbulent mixing layer is fully developed at $x/M_1 = 38.5$.

Large-scale intermittency of velocity fluctuations is evaluated with the flatness $F(u') = \overline{u'^4}/\overline{u'^2}^2$ shown in Fig. 4. $F(u')$ takes a value close to the Gaussian distribution value of 3 in the quasi-homogeneous isotropic turbulent regions and becomes larger than 3 in the mixing layer region, with a peak value of 4.48 at $y = 415$ mm. This peak is on the smaller TKE side from the grid center, which qualitatively agrees with previous studies.[26,30] The velocity fluctuation in the mixing layer region is a combination of the velocity fluctuations in the large and small TKE regions. Since the rate of penetration from the large TKE region is greater, strong intermittent fluctuations appear on the small TKE side from the center.[26] From these results, it is confirmed that the present grid generates the typical shearless turbulent mixing layer with a large-scale intermittency in the mixing layer region.

B. Wavelet analysis

In order to investigate the scale-dependent statistics of the shearless turbulent mixing layer, the discrete wavelet transformation is applied to the signal of u' at $x/M_1 = 38.5$. The LIM $I_{m,n}$ at the large TKE region ($y = 205$ mm), the small TKE region ($y = 475$ mm), and the mixing layer region ($y = 385$ mm) are shown in Fig. 5. Figures 5(a)–5(c) are for $m = 3$, and Figs. 5(d)–5(f) are for $m = 6$. Here, $m = 3$ and $m = 6$ correspond to small and large scales, respectively, and the corresponding scales are listed in Table III. For both small scale ($m = 3$) and large scale ($m = 6$), intermittency is stronger in the mixing layer region. Since Re_λ in the mixing layer region is smaller than that in the large TKE region, the strong intermittency in the mixing layer region is caused by the interaction of turbulence between the small and large TKE regions. Interestingly, the intermittency is more significant at the small scale [Fig. 5(c)] than at the large scale [Fig. 5(f)] in the mixing layer region.

Figure 6 shows the flatness of wavelet coefficients $F(T_m)$ at each vertical position. Here, the wavelet scale m was converted to the spatial scale r with $r = 2^m\overline{U}/f_s$ utilizing Taylor's hypothesis.[35,43,50] Although the flatness changes depending on the scale in all regions, the tendency is quantitatively different. In the quasi-homogeneous isotropic turbulent regions, the flatness becomes asymptotic to 3 faster than in the mixing layer region as the scale r increases. Since the flatness tends to have a larger value at small scales in the large TKE region than in the small TKE region, the small-scale intermittency in the quasi-homogeneous isotropic turbulent regions depends on Re_λ as it should be. On the other hand, in the mixing layer region, the flatness is larger than 3 even at a large scale larger than the mesh width M_1, and the

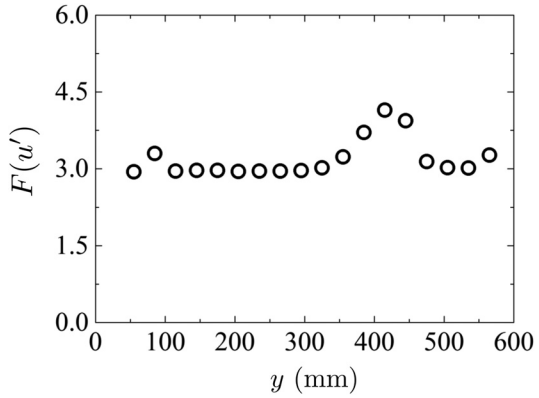

FIG. 4. Vertical distribution of flatness of the streamwise velocity fluctuations.

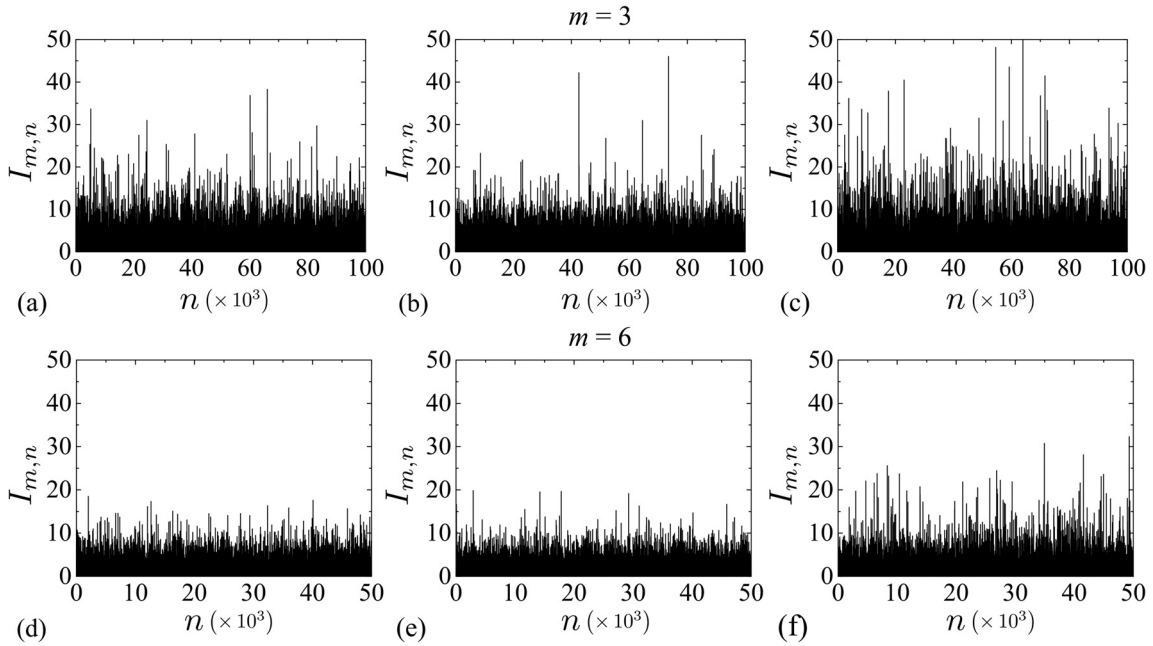

FIG. 5. LIM for $m = 3$: (a) $y = 205$ mm (on the large TKE side); (b) $y = 475$ mm (on the small TKE side); (c) $y = 385$ mm (in the mixing layer). LIM for $m = 6$: (d) $y = 205$ mm; (e) $y = 475$ mm; (f) $y = 385$ mm.

intermittency of turbulent motions at the scale of the mesh width M_1 is also large. Considering that the flatness at a small scale is also larger in the mixing layer region than that in the quasi-homogeneous isotropic turbulent regions and that Re_λ is smaller in the mixing layer region than that in the large TKE region, the large flatness in the mixing layer region is due to inhomogeneity of the flow. Furthermore, it is expected that the interaction of large-scale turbulent motions with small ones may enhance the small-scale intermittency.

C. Conditional statistics

As shown in Sec. III B, we can see the intermittent behavior of velocity fluctuations in a discrete scale m by performing the wavelet transformation. The turbulence signals, therefore, can be divided into two parts with strong and weak intermittency, where fluctuations with weak intermittency are defined to have the flatness factor of 3 for the Gaussian distribution.[40] In order to uniquely determine the threshold, we used the method[40] described in Sec. II B. Figure 7 shows the threshold s obtained by this method. As the threshold s becomes small, the proportion of coefficients with larger energy in signals becomes large, i.e., the stronger intermittency. Comparing the two quasi-homogeneous isotropic turbulent regions, the intermittency is stronger in the large TKE side than that in the small TKE side: the Re_λ dependency on the intermittency in quasi-homogeneous isotropic turbulence is again confirmed. For all scales, intermittency is the strongest in the mixing layer region.

TABLE III. Relationship between m and scale r.

y position (mm)	205	385	475
r ($m = 3$) (mm)	2.32	2.24	2.27
r ($m = 6$) (mm)	18.6	18.0	18.2

Figure 8 shows the ratio of the number of intermittent wavelet coefficients at a certain scale $N(T_{m,n_i})$ to the total number of wavelet coefficients at the same scale $N(T_{m,n})$, where n_i represents the time when $I_{m,n_i} > s$, and Fig. 9 shows the ratio of the energy of intermittent fluctuations at a certain scale E_c^m to the total energy at the same scale E_{tot}^m obtained by

$$E_c^m = \sum_{n_i} T_{m,n_i}^2, \tag{14}$$

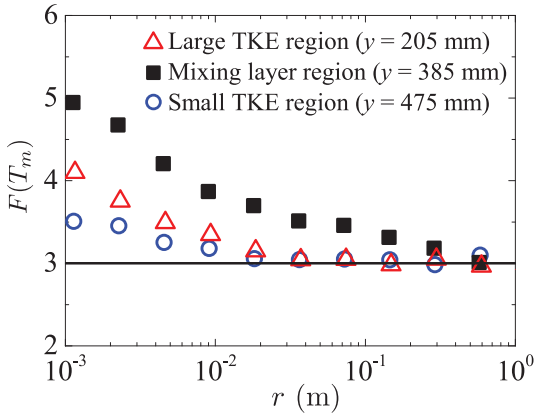

FIG. 6. Flatness of wavelet coefficients.

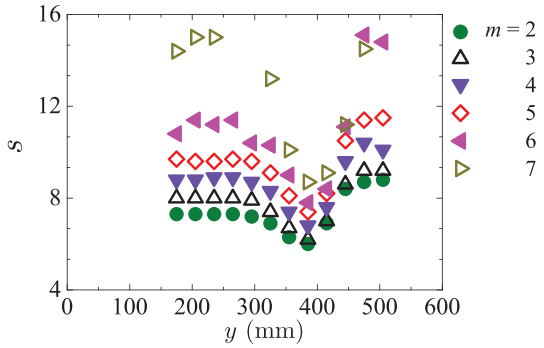

FIG. 7. Vertical distribution of the threshold s for each scale m.

$$E_{tot}^{m} = \sum_{n} T_{m,n}^{2}. \tag{15}$$

In all regions, the number of intermittent wavelet coefficients and the energy increase as the scale decreases. At a small scale, although the number of intermittent wavelet coefficients is a few percent of the total, the total intermittent energy occupies several tens of percent of the total energy. From these results, the threshold successfully divides the wavelet coefficients of turbulent signals into a small number of events with a large amount of energy and most parts of the signal with a little energy whose flatness is 3. Furthermore, the ratios of the number of intermittent coefficients and the energy are larger in the mixing layer region than in the quasi-homogeneous isotropic turbulent regions at all scales.

We also calculate the ratio of E_c^m to the total energy E_{tot}^m when the threshold s is changed.[24] The sum of the total energy E_c^m larger than s of all scales and the total energy E_{tot}^m of all scales,

$$E_c = \sum_{m}\sum_{n_i} T_{m,n_i}^{2}, \tag{16}$$

$$E_{tot} = \sum_{m}\sum_{n} T_{m,n}^{2}, \tag{17}$$

are also calculated. Figures 10(a)–10(c) show the intermittent energy ratio E_c^m/E_{tot}^m for a small scale $m = 3$, a large scale $m = 6$, and the ratio

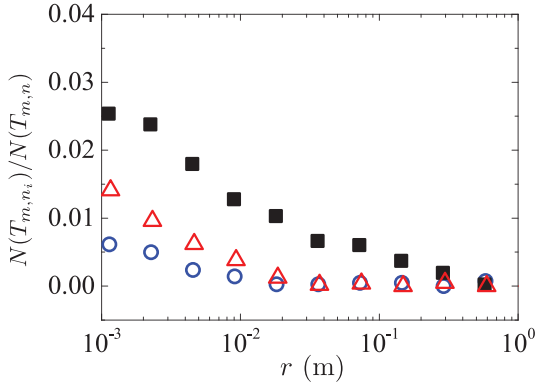

FIG. 8. The ratio of the number of intermittent wavelet coefficients at each scale $N(T_{m,n_i})/N(T_{m,n})$. Symbols as in Fig. 6.

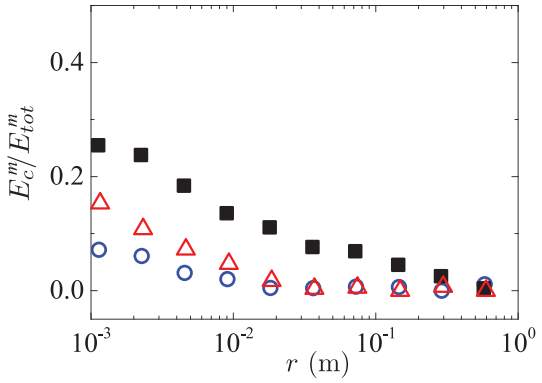

FIG. 9. The ratio of the total energy of intermittent wavelet coefficients at each scale E_c^m/E_{tot}^m. Symbols as in Fig. 6.

of the total of scales E_c/E_{tot} when the threshold s is changed. When s is smaller than 1 in each scale and total, the ratio of fluctuations larger than s is the same regardless of the flow region. At a small scale ($m = 3$), the large TKE region has more intermittent energy than that in the small TKE region for s larger than 1. In the mixing layer region, intermittent energy is much larger than that in the other regions for $s \geq 3$ in each scale. More interestingly, E_c/E_{tot} is also different in the mixing layer region. In the previous study,[24] profiles of E_c/E_{tot} are similar for different Re_λ (i.e., $Re_\lambda \approx 10$ for grid turbulence and $Re_\lambda \approx 800$ for turbulent jet) although the intermittent energy ratio E_c^m/E_{tot}^m at the small scale is quite different. The result suggests that E_c/E_{tot} is not universal but depends on turbulent flows. Note that the discussion of E_c/E_{tot} in Guj and Camussi[24] is limited to locally homogeneous turbulent flows.

In order to investigate the characteristics of signals with strong intermittency, we calculated the scaling exponent $\zeta(p)$ from the wavelet coefficient. Figure 11 shows $2^{-\frac{pm}{2}}\overline{|T_{m,n}|^p}$ ($p = 2$, 4, and 6) vs $2^{-\frac{3m}{2}}\overline{|T_{m,n}|^3}$ at $y = 475$ mm (small TKE region) based on the ESS.[44] The power law relationships are confirmed as in the previous study.[44] The ESS is applied to the original signal and signals with strong and weak intermittency, and $\zeta(p)$ for each signal is obtained by fitting Eq. (13) on scales smaller than the integral scale. The scaling exponents for each case of $p = 1$, 2, 4, 5, and 6 are shown in Figs. 12(a)–12(e). For $p = 1$ and 2, the deviation from K41 is small. On the other hand, the deviations from K41 are obvious for the wavelet coefficient of $p = 4$, 5, and 6 calculated from the original signal (the black square symbols). The scaling exponents of the quasi-homogeneous isotropic turbulent regions have a similar anomalous scaling to those of grid turbulences in previous studies.[21,22] In the case of higher-order scaling exponents, especially $\zeta(6)$, the deviation from K41 is the largest in the mixing layer region. Therefore, the intermittent vortex motion induced by the inhomogeneity of TKE has a larger effect on the higher-order scaling exponent than the effect of the intermittent energy dissipation rate, i.e., effect of Re_λ.

The scaling exponents obtained from the wavelet coefficients with the LIM larger than the threshold s show the effect of strong, intermittent fluctuations. For $p = 1$ and 2, the exponents are almost constant in all regions and are close to the K41 values. For $p = 4$, the deviation from K41 in the mixing layer region becomes clear. This suggests that the deviation from K41 increases depending on the

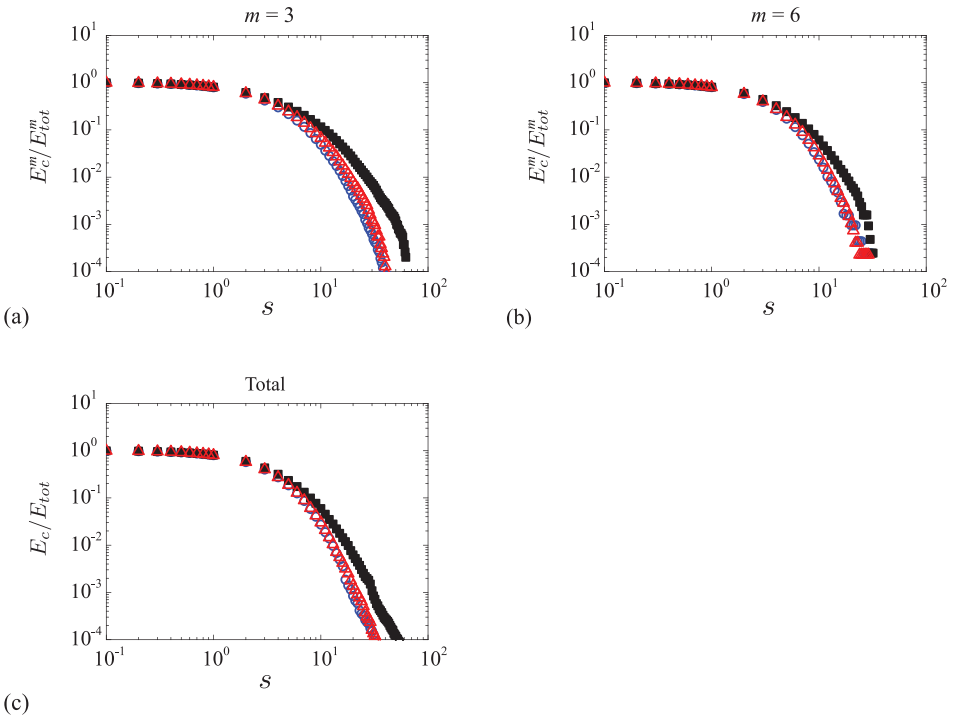

FIG. 10. Intermittent energy ratio E_c^m/E_{tot}^m for (a) m = 3, (b) m = 6, and (c) total of scales E_c/E_{tot}. Symbols as in Fig. 6.

intermittent fluctuations. This tendency is the same for higher-order scaling exponents, and the deviation from K41 is larger in the mixing layer region than in the other regions.

The scaling exponents of the wavelet coefficients with the LIM below s is close to K41 in all regions except in the large TKE region for $p = 6$. This suggests that the anomalous scaling of the original signal in the mixing layer region is caused by strong, intermittent fluctuations, and fluctuations with a wavelet coefficient flatness of 3 may restore the statistical self-similarity shown by the Kolmogorov theory up to $p = 5$ in this flow.[23,24] In other words, even in a flow field with strong intermittency, weak fluctuations with the flatness of 3 have the same universal statistical characteristics as quasi-homogeneous isotropic turbulence at least up to $p = 5$. It should be noted that even for

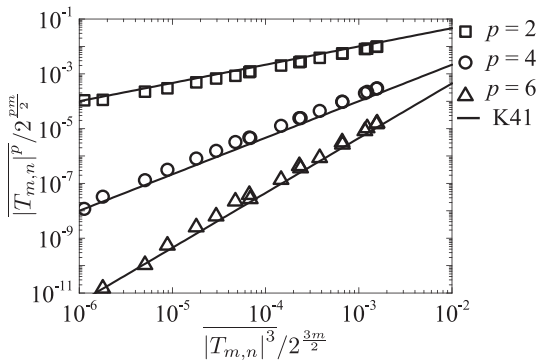

FIG. 11. Wavelet structure functions at y = 475 mm (small TKE region) by ESS.

fluctuations that follow the universal scaling law, the vortex structure is different depending on the flow fields.[23,24] In order to see the effect of threshold value, we calculate the sixth order scaling exponents by giving the same threshold to all scales. Therefore, these thresholds are independent of scale m unlike s. The results are shown in Fig. 12(f). Different symbols in the figure indicate the scaling exponents obtained from the wavelet coefficients with LIMs smaller than the thresholds 1, 5, 10, and 20, respectively. As the threshold becomes smaller, the scaling exponent obtained from the wavelet coefficient with the LIM below the threshold tends to approach the value of K41. Thus, $\zeta(6)$ calculated from the velocity signals with very weak intermittency agrees with the value of K41, and it is inferred that the weak intermittency of fluctuations with a flatness 3 (i.e., smaller than s) still affects $\zeta(6)$.

Camussi and Guj[23] showed that the scaling exponents of the intermittent fluctuations have the similar results regardless of Re_λ (i.e., $Re_\lambda \approx 10$ and 800) and the type of flow fields (i.e., quasi-homogeneous isotropic turbulence and a turbulent jet). In the present shearless turbulent mixing layer, the scaling exponents in the mixing layer region have the different values from the quasi-homogeneous isotropic turbulent region. It is suggested that the scaling exponents can be affected by the presence of intermittent vortex motion. Also, in previous studies in a channel flow and a turbulent boundary layer,[40,41] the scaling exponents deviate from K41 in the buffer layer rather than in the fully turbulent, logarithmic layer. It is inferred that the large deviation from K41 in the buffer layer is due to the presence of coherent structures, which is enhanced by anisotropy.[41] The shearless mixing layer does not have mean velocity shear unlike these flow fields. Despite this, the anisotropy at the small scale may be increased due to the large-scale intermittency,[18] and the scaling exponents change. The investigation

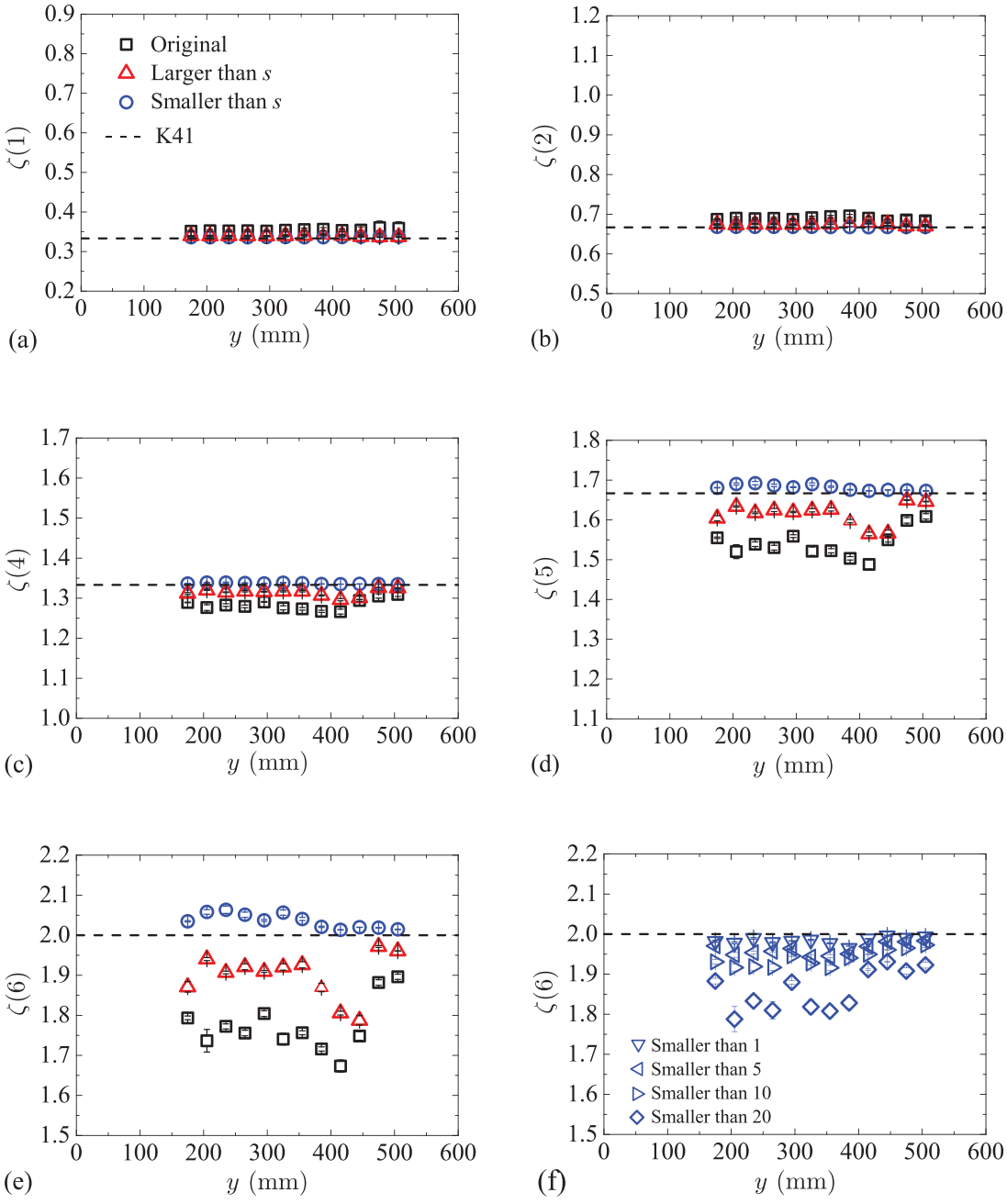

FIG. 12. Vertical profiles of the scaling exponent for (a) $p = 1$, (b) $p = 2$, (c) $p = 4$, (d) $p = 5$, (e) $p = 6$, and (f) $p = 6$ with different thresholds applied to all scales. The uncertainty bars show the root mean square of the deviation from the power function [Eq. (13)].

into the structure of large and small scales in the shearless mixing layer is beyond the scope of this paper, and we leave this issue to a future study.

The deviation of the scaling exponents from the K41 theory may be related to the presence of coherent structures, as described above. Since the coherent structures are intermittent phenomena, their existence can be associated with the LIM $I_{m,n}$.[24] Figures 13(a) and 13(b) show the pdf of $I^{\frac{1}{2}}_{m,n}$ for $m = 3$ (small scale) and $m = 6$ (large scale), respectively. Here, $I^{\frac{1}{2}}_{m,n}$ is introduced by Guj and Camussi[24] and is representative of the velocity difference.[24] For signals with $I^{\frac{1}{2}}_{m,n} < 1$, the probability distributions are similar in all regions for both $m = 3$ and $m = 6$. Therefore, it is suggested that weakly intermittent fluctuations of the flow reach a universal state regardless of Re_λ and strong

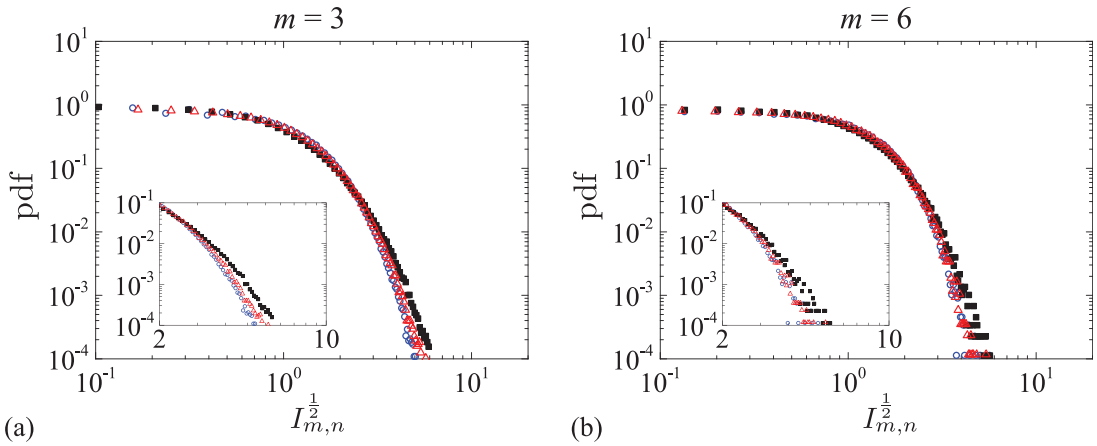

FIG. 13. Pdf of $I^{\frac{1}{2}}_{m,n}$ for (a) $m = 3$ and (b) $m = 6$. Symbols as in Fig. 6.

intermittency when only signals with low intermittency are extracted. On the other hand, for signals with $I^{\frac{1}{2}}_{m,n} > 1$, the large TKE region ($y$ = 205 mm) has higher probability of having a large intermittent energy compared with the small TKE region (y = 475 mm). This tendency is clearer for the small scale (m = 3). In the mixing layer region (y = 385 mm), despite smaller Re_λ than that in the large TKE region, the probability of having a large intermittent energy is larger than that in the large TKE region due to the penetration of vortices from the large TKE region to the small TKE region.

In the shearless turbulent mixing layer, large-scale vortex motions with directivity influence the probability distribution of intermittent energy and cause a behavior different from that in the quasi-homogeneous isotropic turbulent regions. As a result, the scaling exponents in the mixing layer region have values different from those in the quasi-homogeneous isotropic turbulent regions. From this result, for flow fields with strong intermittency such as a shearless turbulent mixing layer, it may be useful to divide the velocity signals into a part that does not depend on the type of flow or Re_λ and a part that depends on the flow field and Re_λ in modeling the energy and its spectrum.

IV. CONCLUSIONS

Intermittency is one of the most important turbulent characteristics, which affects the scaling exponent of the velocity structure function. In previous studies on the scaling exponent in an inhomogeneous flow such as a channel flow, both turbulent production due to mean shear and turbulent diffusion affect the intermittency. In order to split them and focus only on the effect of turbulent diffusion of vortices on anomalous scaling in an inhomogeneous turbulent flow, we experimentally investigate a shearless turbulent mixing layer. A shearless turbulent mixing layer is developed by the interaction of two regions of quasi-homogeneous isotropic turbulence with different TKEs using a parallel bar grid, and the instantaneous streamwise velocity is measured by hot-wire anemometry. Intermittent fluctuations are extracted using the wavelet transformation and their properties are investigated. The threshold for extracting intermittent fluctuations is determined so that the flatness of the wavelet coefficient below the threshold becomes 3. The intermittent properties of the shearless turbulent mixing layer are investigated by obtaining the scaling exponents related to the wavelet coefficient corresponding to the structure function by means of ESS.

The results show that small-scale statistics are strongly affected by large-scale intermittency even without mean shear. In the shearless turbulent mixing layer, the higher-order scaling exponents for intermittent fluctuations in the mixing layer region deviate from the value predicted by the Kolmogorov theory, when compared with the quasi-homogeneous isotropic turbulent region with a larger Re_λ. The mixing layer region in the shearless turbulent mixing layer has strong intermittency, which is caused by the vortex penetration from large to small TKE regions. It is considered that the presence of coherent structures causes the scaling exponents to deviate from the Kolmogorov theoretical value in the shearless turbulent mixing layer. In fact, the LIM obtained by the wavelet analysis confirmed that intermittent motions in the mixing layer region are more active than in the quasi-homogeneous isotropic turbulent regions. Furthermore, the ratio of energy above the threshold to the total energy is considerably larger in the mixing layer region than in other regions, which is different from the previous study for locally homogeneous turbulent flows (i.e., grid turbulence and turbulent jet).[24] The difference may be due to strong inhomogeneity of the present flow. On the other hand, the scaling exponents of weak fluctuations with a wavelet coefficient flatness corresponding to a Gaussian distribution value of 3 follow the Kolmogorov theory up to fifth order. However, the sixth order scaling exponent is still affected by these weak fluctuations. Then, the sixth order scaling exponent approaches the value of K41 for weaker fluctuations with a smaller threshold. From the above results, it is found that turbulent fluctuations consist of weakly intermittent fluctuations that follow a universal statistical law, which is independent on the flow field and Re_λ, and strong intermittent fluctuations, whose statistical properties depend on coherent structures and Re_λ.

Since the scaling law of the velocity structure function is related to the energy transfer from large to small scales,[24] the effects of

inhomogeneity on the scaling exponent and energy transfer in the shearless turbulent mixing layer should further be investigated together with the effects of anisotropy at small scales.[41] The dissipation of TKE in the shearless turbulent mixing layer should also be further investigated. It would be interesting to investigate whether or not the turbulence in the mixing region is non-equilibrium, which has been found in some turbulent flows.[51] It is a future task to investigate the properties of coherent structures of a shearless turbulent mixing layer, which cause the anomalous scaling, and to compare them with other homogeneous/inhomogeneous flows.

ACKNOWLEDGMENTS

This study was supported by the JSPS KAKENHI, Grant No. 18H01367.

DATA AVAILABILITY

The data that support the findings of this study are available from the corresponding author upon reasonable request.

REFERENCES

[1]A. N. Kolmogorov, "The local structure of turbulence in incompressible viscous fluid for very large Reynolds numbers," C. R. Acad. Sci. URSS **30**, 301 (1941).
[2]A. L. Kistler and T. Vrebalovich, "Grid turbulence at large Reynolds numbers," J. Fluid Mech. **26**, 37 (1966).
[3]S. G. Saddoughi and S. V. Veeravalli, "Local isotropy in turbulent boundary layers at high Reynolds number," J. Fluid Mech. **268**, 333 (1994).
[4]G. K. Batchelor and A. A. Townsend, "The nature of turbulent motion at large wave-numbers," Proc. R. Soc. London, Ser. A **199**, 238 (1949).
[5]G. R. Ruetsch and M. R. Maxey, "Small-scale features of vorticity and passive scalar fields in homogeneous isotropic turbulence," Phys. Fluids A **3**, 1587 (1991).
[6]Z.-S. She, E. Jackson, and S. A. Orszag, "Intermittent vortex structures in homogeneous isotropic turbulence," Nature **344**, 226 (1990).
[7]P. Gualtieri, C. M. Casciola, R. Benzi, G. Amati, and R. Piva, "Scaling laws and intermittency in homogeneous shear flow," Phys. Fluids **14**, 583 (2002).
[8]C. M. Casciola, P. Gualtieri, R. Benzi, and R. Piva, "Scale-by-scale budget and similarity laws for shear turbulence," J. Fluid Mech. **476**, 105 (2003).
[9]F. Toschi, G. Amati, S. Succi, R. Benzi, and R. Piva, "Intermittency and structure functions in channel flow turbulence," Phys. Rev. Lett. **82**, 5044 (1999).
[10]F. Coscarella, N. Penna, S. Servidio, and R. Gaudio, "Turbulence anisotropy and intermittency in open-channel flows on rough beds," Phys. Fluids **32**, 115127 (2020).
[11]K. N. Morshed, S. K. Venayagamoorthy, and L. P. Dasi, "Intermittency and local dissipation scales under strong mean shear," Phys. Fluids **25**, 011701 (2013).
[12]E. Rusaouen, B. Chabaud, J. Salort, and P.-E. Roche, "Intermittency of quantum turbulence with superfluid fractions from 0% to 96%," Phys. Fluids **29**, 105108 (2017).
[13]K. R. Sreenivasan and R. A. Antonia, "The phenomenology of small-scale turbulence," Annu. Rev. Fluid Mech. **29**, 435 (1997).
[14]A. N. Kolmogorov, "A refinement of previous hypotheses concerning the local structure of turbulence in a viscous incompressible fluid at high Reynolds number," J. Fluid Mech. **13**, 82 (1962).
[15]C. Meneveau and K. R. Sreenivasan, "Simple multifractal cascade model for fully developed turbulence," Phys. Rev. Lett. **59**, 1424 (1987).
[16]U. Frisch, P.-L. Sulem, and M. Nelkin, "A simple dynamical model of intermittent fully developed turbulence," J. Fluid Mech. **87**, 719 (1978).
[17]T. Gotoh, D. Fukayama, and T. Nakano, "Velocity field statistics in homogeneous steady turbulence obtained using a high-resolution direct numerical simulation," Phys. Fluids **14**, 1065 (2002).
[18]D. Tordella and M. Iovieno, "Small-scale anisotropy in turbulent shearless mixing," Phys. Rev. Lett. **107**, 194501 (2011).
[19]J. Mi and R. Antonia, "Effect of large-scale intermittency and mean shear on scaling-range exponents in a turbulent jet," Phys. Rev. E **64**, 026302 (2001).
[20]A. Attili and F. Bisetti, "Statistics and scaling of turbulence in a spatially developing mixing layer at $Re_\lambda = 250$," Phys. Fluids **24**, 035109 (2012).
[21]A. Arneodo, C. Baudet, F. Belin, R. Benzi, B. Castaing, B. Chabaud, R. Chavarria, S. Ciliberto, R. Camussi, F.Chilla *et al.*, "Structure functions in turbulence, in various flow configurations, at Reynolds number between 30 and 5000, using extended self-similarity," Europhys. Lett. **34**, 411 (1996).
[22]R. Camussi and G. Guj, "Experimental analysis of scaling laws in low Re_λ grid-generated turbulence," Exp. Fluids **20**, 199 (1996).
[23]R. Camussi and G. Guj, "Orthonormal wavelet decomposition of turbulent flows: Intermittency and coherent structures," J. Fluid Mech. **348**, 177 (1997).
[24]G. Guj and R. Camussi, "Statistical analysis of local turbulent energy fluctuations," J. Fluid Mech. **382**, 1 (1999).
[25]B. Gilbert, "Diffusion mixing in grid turbulence without mean shear," J. Fluid Mech. **100**, 349 (1980).
[26]S. Veeravalli and Z. Warhaft, "The shearless turbulence mixing layer," J. Fluid Mech. **207**, 191 (1989).
[27]D. A. Briggs, J. H. Ferziger, J. R. Koseff, and S. G. Monismith, "Entrainment in a shear-free turbulent mixing layer," J. Fluid Mech. **310**, 215 (1996).
[28]B. Knaepen, O. Debliquy, and D. Carati, "Direct numerical simulation and large-eddy simulation of a shear-free mixing layer," J. Fluid Mech. **514**, 153 (2004).
[29]D. Tordella and M. Iovieno, "Numerical experiments on the intermediate asymptotics of shear-free turbulent transport and diffusion," J. Fluid Mech. **549**, 429 (2006).
[30]H. S. Kang and C. Meneveau, "Experimental study of an active grid-generated shearless mixing layer and comparisons with large-eddy simulation," Phys. Fluids **20**, 125102 (2008).
[31]K. Nagata, H. Suzuki, Y. Sakai, T. Hayase, and T. Kubo, "Direct numerical simulation of turbulent mixing in grid-generated turbulence," Phys. Scr. **2008**, 014054.
[32]P. J. Ireland and L. R. Collins, "Direct numerical simulation of inertial particle entrainment in a shearless mixing layer," J. Fluid Mech. **704**, 301 (2012).
[33]J. Jiménez, A. A. Wray, P. G. Saffman, and R. S. Rogallo, "The structure of intense vorticity in isotropic turbulence," J. Fluid Mech. **255**, 65 (1993).
[34]M. Farge, "Wavelet transforms and their applications to turbulence," Annu. Rev. Fluid Mech. **24**, 395 (1992).
[35]G. G. Katul, M. B. Parlange, and C. R. Chu, "Intermittency, local isotropy, and non-Gaussian statistics in atmospheric surface layer turbulence," Phys. Fluids **6**, 2480 (1994).
[36]C. Salem, A. Mangeney, S. D. Bale, and P. Veltri, "Solar wind magnetohydrodynamics turbulence: Anomalous scaling and role of intermittency," Astrophys. J. **702**, 537 (2009).
[37]C. J. Keylock, R. Stresing, and J. Peinke, "Gradual wavelet reconstruction of the velocity increments for turbulent wakes," Phys. Fluids **27**, 025104 (2015).
[38]Z. Tang and N. Jiang, "The effect of a synthetic input on small-scale intermittent bursting events in near-wall turbulence," Phys. Fluids **32**, 015110 (2020).
[39]Y. Yang, W. H. Matthaeus, Y. Shi, M. Wan, and S. Chen, "Compressibility effect on coherent structures, energy transfer, and scaling in magnetohydrodynamic turbulence," Phys. Fluids **29**, 035105 (2017).
[40]M. Onorato, R. Camussi, and G. Iuso, "Small scale intermittency and bursting in a turbulent channel flow," Phys. Rev. E **61**, 1447 (2000).
[41]J. Nan and Z. Jin, "Detecting multi-scale coherent eddy structures and intermittency in turbulent boundary layer by wavelet analysis," Chin. Phys. Lett. **22**, 1968 (2005).
[42]I. Daubechies, *Ten Lectures on Wavelets* (SIAM, 1992).
[43]P. S. Adisson, *The Illustrated Wavelet Transform Handbook: Introductory Theory and Applications in Science, Engineering, Medicine and Finance* (CRC Press, 2002).
[44]R. Benzi, S. Ciliberto, R. Tripiccione, C. Baudet, F. Massaioli, and S. Succi, "Extended self-similarity in turbulent flows," Phys. Rev. E **48**, R29 (1993).
[45]P. E. Roach, "The generation of nearly isotropic turbulence by means of grids," Int. J. Heat Fluid Flow **8**, 82 (1987).
[46]T. Kurian and J. H. M. Fransson, "Grid-generated turbulence revisited," Fluid Dyn. Res. **41**, 021403 (2009).
[47]C. Meneveau, "Analysis of turbulence in the orthonormal wavelet representation," J. Fluid Mech. **232**, 469 (1991).

[48]G. Beylkin, R. Coifman, and V. Rokhlin, "Fast wavelet transforms and numerical algorithms I," Commun. Pure Appl. Math. **44**, 141 (1991).
[49]M. Yamada and K. Ohkitani, "Orthonormal wavelet analysis of turbulence," Fluid Dyn. Res. **8**, 101 (1991).
[50]H. Mouri, H. Kubotani, T. Fujitani, H. Niino, and M. Takaoka, "Wavelet analyses of velocities in laboratory isotropic turbulence," J. Fluid Mech. **389**, 229 (1999).
[51]J. C. Vassilicos, "Dissipation in turbulent flows," Annu. Rev. Fluid Mech. **47**, 95 (2015).